PHYSICAL REVIEW B **71**, 041309(R) (2005)

$[\bar{1}100]/(1102)$ twin boundaries in wurtzite ZnO and group-III-nitrides

Yanfa Yan and M. M. Al-Jassim
National Renewable Energy Laboratory, Golden, Colorado 80401, USA

M. F. Chisholm, L. A. Boatner, and S. J. Pennycook
Oak Ridge National Laboratory, Oak Ridge, Tennessee 37831, USA

M. Oxley
School of Physics, University of Melbourne, Victoria 3010, Australia
(Received 10 November 2004; published 28 January 2005)

The atomic structure and electronic effects of the $[\bar{1}100]/(1102)$ twin boundary in ZnO are studied using the combination of high-resolution *Z*-contrast imaging, first-principles density-functional total-energy calculations, and image simulations. The twin boundary is found to have the head-to-tail polarity configuration, which avoids dangling bonds, leading to a low twin-boundary energy of 0.040 J/m^2. We further find that the same twin boundaries in wurtzite group-III-nitrides adopt the same structure, but the twin-boundary energies, 0.109 J/m^2 in AlN, 0.107 J/m^2 in GaN, and 0.051 J/m^2 in InN, are higher than in ZnO. Investigations of the electronic structure reveal that the twin boundary does not introduce localized energy states in the band gap in either ZnO or the wurtzite group-III-nitrides.

DOI: 10.1103/PhysRevB.71.041309 PACS number(s): 61.72.Mm, 68.37.Lp, 61.72.Bb

ZnO has long been recognized as a useful material for optically transparent conducting layers in displays and photovoltaic devices.[1–3] Recently, it was realized that ZnO could be an ideal material for low-cost light-emitting diodes and lasers because of its large exciton binding energy and the availability of large-area ZnO substrates.[4–6] So far, most ZnO thin films and bulk crystals are found to contain a high density of extended defects, such as stacking faults, dislocations, and twin boundaries.[7] The extended defects are known to play an important role in electronic and mechanical properties of semiconductors. For example, these defects may introduce electrically active energy levels in the band gap.[8,9] In that case, the quantum efficiencies and device lifetime can be affected. In ZnO, the structure and effects of some extended defects, e.g., [0001] tilt boundaries, stacking faults, and inversion domain boundaries, have been investigated.[10–12] It has been reported that in bulk ZnO synthesis, $[\bar{1}100]/(1102)$ twin boundaries are often present, resulting in zigzagged morphology.[13] However, the structure and effects of the $[\bar{1}100]/(1102)$ twin boundary have not yet been studied.

In this paper, we present our studies on the atomic structure and electronic effects of the $[\bar{1}100]/(1102)$ twin boundaries in wurtzite ZnO using the combination of high-resolution *Z*-contrast imaging, first-principles density-functional total-energy calculations, and image simulation. We find that the $[\bar{1}100]/(1102)$ twin boundary has a head-to-tail polarity configuration, which avoids dangling bonds, leading to a low twin-boundary energy of 0.040 J/m^2. We further find that the head-to-tail polarity configuration can be more generally adopted for this twin boundary in other wurtzite materials, such as the group-III-nitrides. However, the twin-boundary energies, 0.109 J/m^2 in AlN, 0.107 J/m^2 in GaN, and 0.051 J/m^2 in InN, are higher than in ZnO. These results suggest that the $[\bar{1}100]/(1102)$ twin boundary is easier to form in ZnO and InN than in AlN and GaN. Investigations of the electronic structure reveal that the twin boundary does not introduce localized energy states in the band gap in either ZnO or the wurtzite group-III-nitrides.

High-resolution *Z*-contrast imaging was performed using a VG Microscopes HB603U scanning transmission electron microscope operating at 300 kV. The *Z*-contrast images were formed by scanning a 1.26-Å probe across a specimen and recording the transmitted high-angle scattering with an annular detector (inner angle ~45 mrad). The image intensity can be described approximately as a convolution between the electron probe and an object function. Thus, the *Z*-contrast image gives a directly interpretable, atomic resolution map of the columnar scattering cross section in which the resolution is limited by the size of the electron probe.[14,15]

Our first-principles density-functional total-energy calculations are based on the density-functional theory, using the Vienna *ab initio* simulation package (VASP).[16] We used the local-density approximation for the exchange correlation and ultrasoft Vanderbilt-type pseudopotentials[17] as supplied by Kresse and Hafner.[18] The Zn 3*d* electrons were treated as part of the valence band. The cutoff energy for the plane-wave basis was 400 eV. The twin boundaries are modeled with supercells. A 64-host-atom supercell was used for twin-boundary energy calculations. In all calculations, all atoms were allowed to relax to reach the minimum energies until the Hellmann-Feynman forces acting on them became less than 0.02 eV/Å.

Z-contrast imaging. Figure 1 shows a *Z*-contrast image of a $[\bar{1}100]/(1102)$ twin boundary in ZnO along the $[\bar{1}100]$ zone axis. The twin boundary is indicated by the white dashed line. Each bright spot in this image is the projection of a single column of Zn atoms. The distance between a Zn

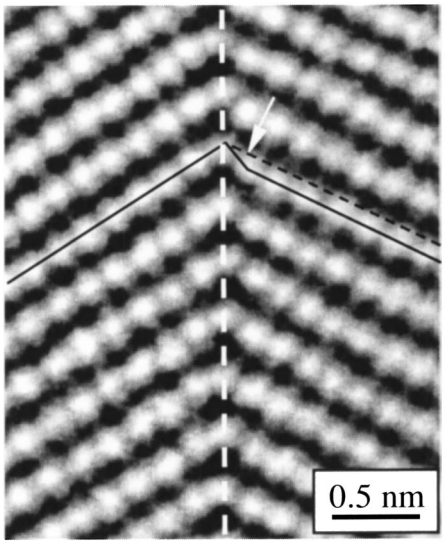

FIG. 1. *Z*-contrast image of a $[\bar{1}100]/(1102)$ twin boundary in ZnO along the $[\bar{1}100]$ zone axis.

column and its nearest O column in the bulk in this projection is only 0.61 Å; hence, the O columns cannot be resolved, but the bright Zn columns in the *Z*-contrast image clearly exhibit an elongated shape due to the closely spaced O columns. The two black solid lines indicate a (0002) plane at each side of the boundary. It is seen, interestingly, that the two sides of the boundary are not mirror images, which is what one would expect from a simple twinning operation. The two planes have a relative shift along the twin boundary. This is clear by comparing the black solid line and the black dashed line in the right-hand side of the twin boundary. The black dashed line is in the ideal twin position of the black solid line in the left-hand side of the twin boundary.

Twin-boundary structures. ZnO is a polar crystal; therefore, a $[\bar{1}100]/(1102)$ twin boundary can have three possible polarity configurations, namely a head-to-tail ($\searrow|\nearrow$), a head-to-head ($\searrow|\swarrow$), and a tail-to-tail ($\nwarrow|\nearrow$) configuration, where the arrows indicate the polarity (the direction from the O atoms to the Zn atoms along the O-Zn bonds parallel to the *c* axis) and the $|$ symbol indicates the twin-boundary plane. In the first configuration, the polarities on the two sides of the boundary do not exhibit a mirror relation across the boundary plane. However, in the second and third configurations, the two sides do exhibit a mirror relation across the boundary plane. These three polarity configurations result in different atomic structures for the twin boundary.

We then construct the atomic structures for the $[\bar{1}100]/(1102)$ twin boundary with these three possible polarity configurations. These structures are then relaxed by first-principles total-energy calculations. Figures 2(a)–2(c) show the three relaxed structures for the head-to-tail ($\searrow|\nearrow$), head-to-head ($\searrow|\swarrow$), and tail-to-tail ($\nwarrow|\nearrow$) configurations, respectively. The arrows in Fig. 2 indicate the polarities and the dashed lines indicate the boundary planes. The black balls denote O atoms, whereas the gray balls denote Zn atoms. None of these three structures contain any Zn-Zn or O-O wrong bonds. In the structure shown in Fig. 2(a), both the Zn and O atoms in the boundary are fourfold coordinated, the same as in ZnO bulk. Thus, there is no dangling bond in the boundary. However, the bond angles in the boundary are different from that in the bulk. In the structure shown in Fig. 2(b), the Zn and O atoms in the boundary are fivefold and threefold coordinated, respectively. In the structure shown in Fig. 2(c), the Zn and O atoms in the boundary are threefold and fivefold coordinated, respectively. Thus, in the structures shown in Figs. 2(b) and 2(c), there are both dangling bonds and wrong bond angles. Indeed, as we will see later, our first-principles total-energy calculations reveal that the structure shown in Fig. 2(a) has much lower boundary energy than the other two structures.

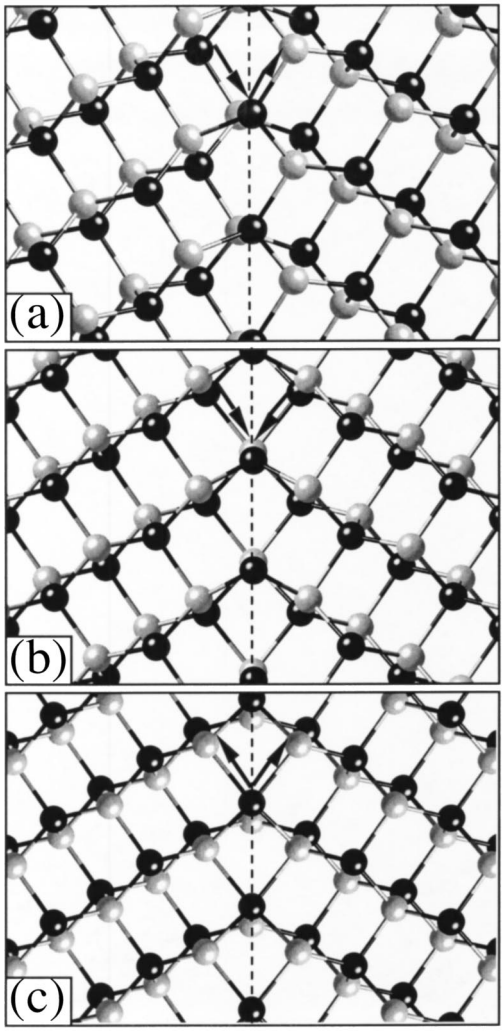

FIG. 2. Fully relaxed structures for the (a) head-to-tail, (b) head-to-head, and (c) tail-to-tail configurations. The arrows indicate the polarities and the dashed lines indicate the boundary planes. The black balls denote O atoms, whereas the grey balls denote Zn atoms.

The wurtzite ZnO structure consists of Zn and O sublattices. A (0002) plane contains a (0002)-Zn subplane and a (0002)-O subplane. In the structures shown in Figs. 2(b) and 2(c), both the (0002)-Zn subplane and the (0002)-O subplane at the left-hand side and their counterparts at the right-

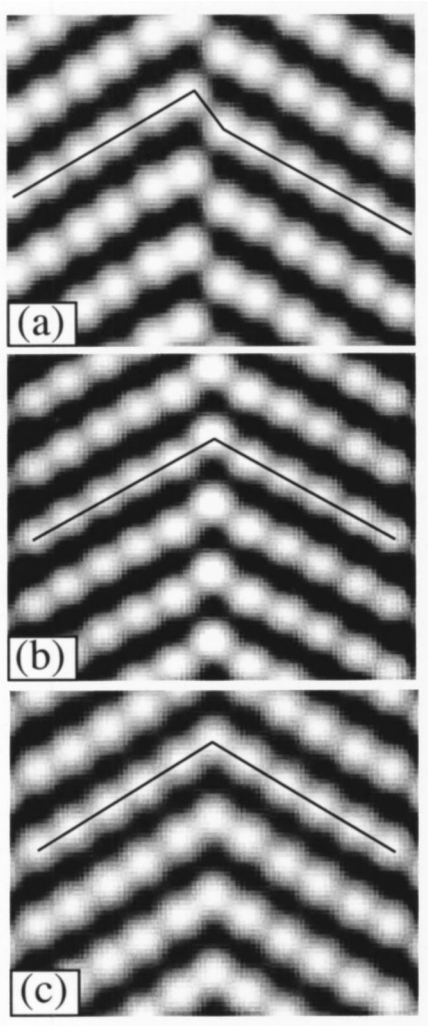

FIG. 3. Simulated *Z*-contrast images using the (a) head-to-tail, (b) head-to-head, and (c) tail-to-tail structures.

hand side are at the mirror positions. However, in the structure shown in Fig. 2(a), the (0002)-Zn subplane at the left-hand side is at the mirror position of the (0002)-O subplane at the left-hand side. Thus, the (0002)-Zn subplanes at two sides of the boundary have a relative shift according to their ideal twin positions. This would explain the feature observed in the *Z*-contrast image, i.e., the two (0002) planes have a relative shift along the twin boundary, because the contribution to the image from the (0002)-O plane is very small. This is shown to be the best-fit structure by *Z*-contrast image simulations. Figures 3(a)–3(c) show the simulated *Z*-contrast images using the corresponding structures shown in Figs. 2(a)–2(c). The parameters used in the simulations are: $C_s=1.0$ mm, $\Delta f=-512$ Å, corresponding to a probe size of 1.3 Å, dark-field detector angle =45–140 mrads, and sample thickness =50 Å. We see that only Fig. 3(a) shows a shift along the boundary, but Figs. 3(b) and 3(c) show ideal twins. The good agreement between Fig. 3(a) and the *Z*-contrast image suggests that the $[1\bar{1}00]/(1102)$ twin boundary in ZnO has the head-to-tail structure shown in Fig. 2(a).

Energetics. The twin-boundary energy for the head-to-tail structure is calculated by $E_{TB}=(E-E_{\text{bulk}})/2A$, where E is the total energy of a supercell containing two boundaries, E_{bulk} is the total energy of a reference supercell with bulk structure and with an equivalent number of atoms, and A is the area of the periodic unit cell of the boundary. In this case, the supercell has the structure of $\searrow|\nearrow|\searrow$, containing two equivalent but oppositely oriented boundaries. For the head-to-head and tail-to-tail structures, it is not possible to construct a repeatable supercell to contain only one of these two structures. A repeatable supercell always contains both of these two structures, giving a repeatable structure as $\searrow|\swarrow|\searrow$. Thus, the total boundary energy is calculated by $E_{TB}=(E-E_{\text{bulk}})/A$. The boundary-energy difference between these two structures is calculated using slabs isolated by a vacuum gap of 20 Å. The periodically repeated supercells and the isolated slab supercells give the same relaxed structures for both head-to-head and tail-to-tail configurations. The boundary energy for each of these configurations can then be calculated from the boundary-energy difference and total boundary energy.

The calculated boundary energies are 0.040 J/m^2 for the head-to-tail configuration, 0.154 J/m^2 for the head-to-head configuration, and 0.118 J/m^2 for the tail-to-tail configuration. The boundary energy for the head-to-tail configuration is significantly lower than for the other two configurations, supporting the conclusion from image simulations that the $[1\bar{1}00]/(1102)$ twin boundary should have the structure shown in Fig. 2(a). The boundary energy for the head-to-tail structure is comparable to the formation energies of inversion domain boundaries (0.043 J/m^2) and stacking faults (0.027 J/m^2 for intrinsic and 0.084 J/m^2 for extrinsic) in ZnO. Thus, the $[1\bar{1}00]/(1102)$ twin boundary is expected to form as easily as the inversion domain boundaries and stacking faults in ZnO.

Electronic effects. The electronic structures of these three structures are investigated. We find that the head-to-head and tail-to-tail structures introduce localized states in the band gap, because these two structures introduce dangling bonds at the boundaries. The head-to-tail structure shown in Fig. 2(a) does not introduce any energy level in the band gap, mainly because this structure does not have any dangling bonds. However, we find that this structure causes a slight shift of the conduction-band minimum (CBM) and the valence-band maximum (VBM) at Γ. To understand whether these shifted CBM and VBM states are localized or not, we plotted the plane-averaged charge density of the CBM and VBM states along the direction perpendicular to the boundary. Figures 4(a) and 4(b) show the plane-averaged charge density of the CBM and VBM states, respectively. The position of the twin boundary is indicated by the dotted line. We see that for both the CBM and VBM states, the localization effect is very weak. Thus, this twin boundary should be electrically inactive, unless high-concentration impurities segregate into the boundary.

Comparison with wurtzite III-nitrides. The wurtzite group-III-nitrides, such as AlN, GaN, and InN, are very attractive materials because of their potential for optoelectronic devices. They have the same structure as ZnO. In fact, many extended defects found in these nitrides are very similar to those found in ZnO.[12,19,20] For example, the formation energies are comparable for inversion domain boundaries

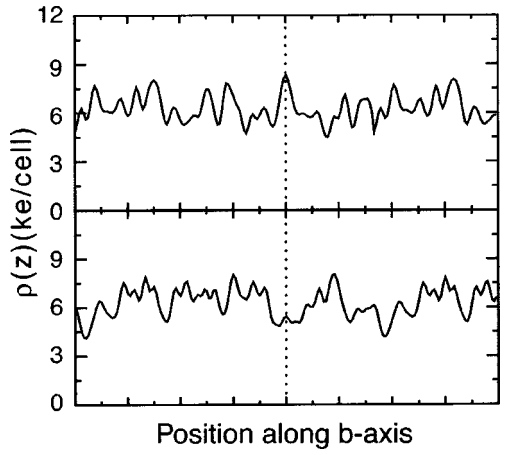

FIG. 4. Plane-averaged charge densities for (a) CBM and (b) VBM along the direction perpendicular to the boundary. The dotted lines indicate the positions of the twin boundaries.

and stacking faults in GaN and ZnO. We find that the $[1\bar{1}00]/(1102)$ twin boundaries in these wurtzite group-III-nitrides also adopt the head-to-tail structure. We thus calculated the boundary energies in these wurtzite group-III-nitrides. The comparison of the boundary energies is given in Table I. We see that the boundary energy is significantly lower in ZnO and InN than in AlN and GaN. This result suggests that the $[1\bar{1}00]/(1102)$ twin boundary is expected to form more easily in ZnO and InN than in AlN and GaN. Investigations of their electronic structures reveal that as in ZnO, this twin boundary does not introduce any energy states in the band gap in these III-nitrides.

TABLE I. Calculated twin-boundary energies (in J/m^2) for the $[1\bar{1}00]/(1102)$ twin boundary in ZnO, AlN, GaN, and InN.

	ZnO	AlN	GaN	InN
E_{TB}	0.040	0.109	0.107	0.051

In conclusion, we have studied the atomic structure and effects of the $[1\bar{1}00]/(1102)$ twin boundary in ZnO using the combination of high-resolution *Z*-contrast imaging, first-principles density-functional total-energy calculations, and image simulations. We found that the twin boundary exhibits the head-to-tail configuration, which avoids dangling bonds, leading to a low twin-boundary energy of 0.040 J/m^2. We further found that the head-to-tail polarity configuration can be more generally adopted for this twin boundary in other wurtzite materials, such as the group-III-nitrides. However, the twin-boundary energies, 0.109 J/m^2 in AlN, 0.107 J/m^2 in GaN, and 0.051 J/m^2 in InN, are higher than in ZnO. Investigations of the electronic structure reveal that the twin boundary does not introduce localized energy states in the band gap in both ZnO and the wurtzite group-III-nitrides.

The *ab initio* total-energy and molecular-dynamics package, Vienna *ab initio* simulation package, was developed at the Institute für Theoretische Physik of the Technische Universität Wien. Work at NREL and ORNL was supported by the U.S. Department of Energy under Contracts No. DE-AC36-99GO10337 and DE-AC05-00OR22725. This research used resources of the National Energy Research Scientific Computing Center, which is supported by the Office of Science of the U.S. Department of Energy under Contract No. DE-AC03-76SF00098.

[1] J. R. Tuttle, M. A. Contreras, T. J. Gillespie, K. R. Ramanathan, A. L. Tennant, J. Keane, A. M. Gabor, and R. Noufi, Prog. Photovoltaics **3**, 235 (1995).
[2] H. J. Ko, Y. F. Chien, S. K. Hong, H. Wenisch, T. Yao, and D. C. Look, Appl. Phys. Lett. **77**, 3761 (2000).
[3] X. L. Guo, J. H. Choi, H. Tabata, and T. Kawai, Jpn. J. Appl. Phys., Part 1 **40**, L177 (2001).
[4] Y. Segawa, A. Ohtomo, M. Kawasaki, H. Koinuma, Z. K. Tang, P. Yu, and G. K. L. Wong, Phys. Status Solidi B **202**, 669 (1997).
[5] D. M. Bagnall, Y. F. Chen, Z. Zhu, T. Yao, M. Y. Shen, and T. Goto, Appl. Phys. Lett. **73**, 1038 (1998).
[6] R. L. Hoffman, B. J. Norris, and J. F. Wager, Appl. Phys. Lett. **82**, 733 (2003).
[7] D. Gerthsen, D. Litivinov, Th. Gruber, C. Kirchner, and A. Waag, Appl. Phys. Lett. **81**, 3972 (2002).
[8] H. Iwata, U. Lindefelt, S. Oberg, and P. R. Briddon, Phys. Rev. B **65**, 033203 (2003).
[9] H. Iwata, U. Lindefelt, S. Oberg, and P. R. Briddon, J. Appl. Phys. **93**, 1577 (2003).
[10] F. Oba, S. R. Nishitami, H. Adachi, I. Tanaka, M. Kohyama, and S. Tanaka, Phys. Rev. B **63**, 045410 (2001).
[11] F. Oba, H. Ohta, Y. Sato, H. Hosono, T. Yamamoto, and Y. Ikuhara, Phys. Rev. B **70**, 125415 (2004).
[12] Y. Yan and M. M. Al-Jassim, Phys. Rev. B **69**, 085204 (2004).
[13] L. A. Boatner (unpublished).
[14] S. J. Pennycook and D. E. Jesson, Phys. Rev. Lett. **64**, 938 (1990).
[15] S. J. Pennycook and P. D. Nellist, J. Microsc. **190**, 159 (1998).
[16] G. Kresse and J. Hafner, Phys. Rev. B **47**, 558 (1993); **49**, 14 251 (1994); G. Kresse and J. Furthmüller, *ibid.* **54**, 11 169 (1996).
[17] D. Vanderbilt, Phys. Rev. B **41**, 7892 (1990).
[18] G. Kresse and J. Hafner, J. Phys.: Condens. Matter **6**, 8245 (1994).
[19] J. E. Northrup, J. Beugebauer, and L. T. Romano, Phys. Rev. Lett. **77**, 103 (1996).
[20] C. Stampfl and C. G. Van de Walle, Phys. Rev. B **57**, R15 052 (1998).